(Pyrazolato)gold Complexes Showing Room-Temperature Columnar Mesophases. Synthesis, Properties, and Structural Characterization

Joaquín Barberá,[†] Anabel Elduque,[‡] Raquel Giménez,[†] Fernando J. Lahoz,*[,‡] José A. López,[‡] Luis A. Oro,*[,‡] and José L. Serrano*[,†]

Departamento de Química Inorgánica and Departamento de Química Orgánica, Instituto de Ciencia de Materiales de Aragón, Universidad de Zaragoza-Consejo Superior de Investigaciones Científicas, 50009 Zaragoza, Spain

Received December 30, 1997

Mesogenic (pyrazolato)gold complexes of formula $[Au(pz)]_3$ (pz = 3,5-bis(3′,4′-di-*n*-decyloxyphenyl)pyrazole (**1**), 3-(3′,4′,5′-tri-*n*-decyloxyphenyl)-5-(3″,4″-di-*n*-decyloxyphenyl)pyrazole (**2**), 3-(2′,3′,4′-tri-*n*-decyloxyphenyl)-5-(3″,4″,5″-tri-*n*-decyloxyphenyl)pyrazole (**3**), 3,5-bis(3′,4′,5′-tri-*n*-decyloxyphenyl)pyrazole (**4**)) have been prepared by reaction of the potassium salts of the nonmesogenic pyrazolate ligands with [AuCl(tht)] (tht = tetrahydrothiophene) in a 1:1 molar ratio. All these compounds show columnar mesophases that remain stable, at room temperature, for long periods of time. The formation of isomers for the nonsymmetrical derivatives—detected by spectroscopic studies—are suggested to be responsible for the subtle changes observed in the transition temperatures. Powder X-ray diffraction measurements show clearly that the supramolecular columnar arrangement appears in the crystalline solids as well as in the mesomorphic phase. An analogue of the mesogenic trinuclear complexes **1**−**4**, having a methoxy group at the phenyl substituents of the pyrazolate ligands, $[Au\{3,5\text{-}(MeOPh)_2Pz\}]_3$ (**5**), has been synthesized and characterized by an X-ray single-crystal diffraction experiment. The molecular structure of **5** is based on a nine-membered metallacycle core. The whole molecule exhibits a rough planarity that favors a crystalline structure formed from columnar arrangements of trinuclear complexes. A simple and clear relationship could be established between the solid-state crystal structure of **5** and the X-ray-deduced structure of the mesophases.

Introduction

In recent years, a new area of vigorous research has appeared in the liquid crystals field: *metallomesogens* (metal-containing liquid crystals).[1] An important aspect in the development of metallomesogens has been the tailored synthesis of columnar superstructures.[2] The use of simple organic nonmesogenic molecules as subunits, and metals or metalloids as links, has allowed the construction of new molecular structures fulfilling the geometric requirements to stack in columns.[3] This approach has been reinforced by the potential technological applications of these columnar supramolecular systems in the fields of photonics, electronics, and ionic transport.[4] This strategy has been applied in the literature to obtain several series of mononuclear or dinuclear metallomesogenic complexes derived from β-diketonate and other related ligands with different transition metals (such as Cu, Ni, Pd, V, Tl, Fe, Mn, and Cr).[1] However no columnar structures had been previously investigated bearing trinuclear central cores and only a few cases of liquid crystals have been described containing gold atoms.[5]

We now present new trinuclear gold complexes displaying interesting mesomorphic properties prepared from nonmesogenic pyrazolate ligands. The choice of these ligands is based on the well-known ability of azolates to yield di-, tri-, tetra-, hexa-, or octanuclear complexes containing metal centers, such as rhodium,[6] iridium,[7] copper,[8,9] silver,[8] or gold,[8,10] joined by one or two exobidentate ligands.[11] Additionally, with the exception of a related work on mesogenic pyrazaboles,[12] pyrazolate-based

[†] Departamento de Química Orgánica.
[‡] Departamento de Química Inorgánica.

(1) (a) Serrano, J. L., Ed. *Metallomesogens. Synthesis, Properties and Applications*; VCH: Weinheim, Germany, 1996. (b) Hudson, S. A.; Maitlis, P. M. *Chem. Rev.* **1993**, *93*, 861. (c) Espinet, P.; Esteruelas, M. A.; Oro, L. A.; Serrano, J. L.; Sola, E. *Coord. Chem. Rev.* **1992**, *117*, 215. (d) Bruce, D. W. In *Inorganic Materials*, 2nd ed.; Bruce, D. W., O'Hare, D., Eds.; John Wiley & Sons: Chichester, U.K., 1996; Chapter 8. (e) Giroud-Godquin, A. M.; Maitlis, P. M. *Angew. Chem., Int. Ed. Engl.* **1991**, *30*, 375. (f) Polishchuk, A. P.; Timofeeva, T. V. *Russ. Chem. Rev. (Engl. Transl.)* **1993**, *62*, 291.

(2) Barberá, J. In ref 1a, Chapter 4.

(3) (a) Giroud-Godquin, A. M.; Gauthier, M. M.; Sigaud, G.; Hardouin, F.; Achard, M. F. *Mol. Cryst. Liq. Cryst.* **1986**, *132*, 35. (b) Ohta, K.; Ema, H.; Muroki, H.; Yamamoto, I.; Matsuzaki, K. *Mol. Cryst. Liq. Cryst.* **1987**, *147*, 61. (c) Zheng, H.; Carroll, P. J.; Swager, T. M. *Liq. Cryst.* **1993**, *14*, 1421. (d) Atencio, R.; Barberá, J.; Cativiela, C.; Lahoz, F. J.; Serrano, J. L.; Zurbano, M. M. *J. Am. Chem. Soc.* **1994**, *116*, 11558. (e) Ibn-Elhaj, M.; Guillon, D.; Skoulios, A.; Giroud-Godquin, A. M.; Maldivi, P. *Liq. Cryst.* **1992**, *11*, 731. (f) Baxter, D. V.; Cayton, R. H.; Chisholm, M. H.; Huffman, J. C.; Putilina, E. F.; Tagg, S. L.; Wesemann, J. L.; Zwanziger, J. W.; Darrington, F. D. *J. Am. Chem. Soc.* **1994**, *116*, 4551. (g) Barberá, J.; Esteruelas, M. A.; Levelut, A. M.; Oro, L. A.; Serrano, J. L.; Sola, E. *Inorg. Chem.* **1992**, *31*, 732.

(4) (a) Ros, M. B. In ref 1a, Chapter 11. (b) Zerbi, G., Ed. *Organic Materials for Photonics;* European Materials Research Society Monographs 6; North-Holland: Amsterdam, 1993. (c) Matsumoto, M.; Tachibana, H.; Nakamura, T. In *Organic Conductors: Fundamentals and Applications*; Farges, J. P., Ed.; Marcel Dekker: New York, 1994; Chapter 16. Di Marco, P.; Giro, G. Ibid., Chapter 17. (d) Carter, F. L., Ed. *Molecular Electronics Devices*; Marcel Dekker: New York, 1982.

(5) (a) Coco, S.; Espinet, P.; Martín-Alvarez, J. M.; Levelut, A. M. *J. Mater. Chem.* **1997**, *7*, 19. (b) Bruce, D. W.; Lalinde, E.; Styring, P.; Dunmur, D. A. *J. Chem. Soc., Chem. Commun.* **1986**, 581. (c) Adams, H.; Albéniz, A. C.; Bailey, N. A.; Bruce, D. W.; Cherodian, A. S.; Dhillon, R.; Dunmur, D. A.; Espinet, P.; Feijoo, J. L.; Lalinde, E.; Maitlis, P. M.; Richardson, R. M.; Ungar, G. *J. Mater. Chem.* **1991**, *1*, 843. (d) Kaharu, T.; Ishii, R.; Takahashi, S. *J. Chem. Soc., Chem. Commun.* **1994**, 1349. (e) Zhang, S. W.; Ishii, R.; Takahashi, S. *Organometallics* **1997**, *16*, 1349.

S0020-1669(97)01632-7 CCC: $15.00
Published on Web 06/15/1998

molecules have not been used as organic ligands to generate mesogenic complexes.

On the basis of our previous studies with related boron-containing derivatives,[12] we have selected as intermetallic bridging ligands the pyrazolate groups estimated to have the best possibilities to generate mesomorphism. They present, in the 3- and 5-positions of the azolate rings, two phenyl groups each substituted with two or three aliphatic (decyloxy) chains.

In this paper, we report the detailed synthetic procedure for the preparation of the first disklike metallomesogens based on trinuclear (pyrazolato)gold complexes which exhibit mesogenic behavior in the proximity of room temperature, together with the X-ray powder diffraction studies of the mesomorphic and solid-state (powder) phases. Along with the investigation of the liquid crystal properties, a single-crystal X-ray analysis of a short-chain homologue, tris[3,5-bis(4′-methoxyphenyl)pyrazolato]trigold(I), has been carried out to obtain insight into the molecular structures and packing arrangements of these compounds in the crystalline phase. Furthermore, we have related the structural information obtained from the different phases in order to understand the role of molecular interactions in the mesogenic behavior.

Part of this work has been reported in a preliminary communication.[13]

Results and Discussion

Complexes of general formula $[Au(pz)]_3$ have been prepared by reaction of the potassium salts of the nonmesogenic pyrazolate ligands with [AuCl(tht)] (tht = tetrahydrothiophene):

$$3[AuCl(tht)] + 3Kpz \rightarrow [Au(pz)]_3 + 3KCl + 3tht \quad (1)$$

For $[Au(pz)]_3$, pz = 3,5-bis(3′,4′-di-*n*-decyloxyphenyl)pyrazole (**1**), 3-(3′,4′,5′-tri-*n*-decyloxyphenyl)-5-(3″,4″-di-*n*-decyloxyphenyl)pyrazole (**2**), 3-(2′,3′,4′-tri-*n*-decyloxyphenyl)-5-(3″,4″,5″-tri-*n*-decyloxyphenyl)pyrazole (**3**), and 3,5-bis(3′,4′,5′-tri-*n*-decyloxyphenyl)pyrazole (**4**). The nuclearity of the complexes has been confirmed by molecular weight and mass spectrometry measurements.

Chart 1

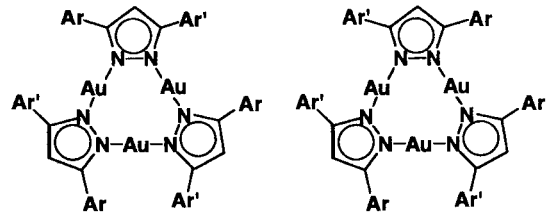

Isomer a Isomer b

Compound	Ar	Ar′
1	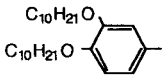	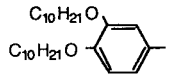
2	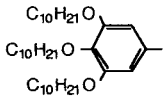	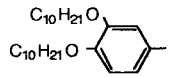
3	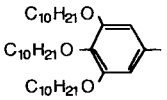	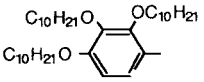
4	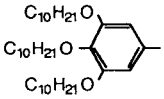	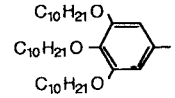

* Compounds **1** and **4** do not lead to isomers.

Complexes **1**−**4** have also been characterized by NMR spectroscopy. The ^{1}H NMR spectra of compounds **1** and **4** indicate the formation of only one isomer, with a D_{3h} symmetry, as a consequence of the rotation of the aromatic rings around the C(pyrazolate)−C(phenyl) bond in solution.

On the other hand, compounds **2** and **3**, which contain two differently substituted aromatic rings in the pyrazolate groups (Ar and Ar′ in Chart 1), exhibit more complicated ^{1}H NMR spectra. Four different signals have been detected for each hydrogen atom directly bonded to the pyrazolate rings and to the phenyl groups. Curiously, for compound **2** the four signals have similar integration values. The explanation of these spectra is based on the existence of two different geometrical isomers statistically obtained in a 1:3 ratio.[13] One type of isomer exhibits a C_{3h} symmetry (isomer a, Chart 1), implying a magnetic equivalence of the substituents in 3- and 5-positions of the pyrazolate rings, respectively, and the other one presents an asymmetric disposition of the pyrazolate substituents (isomer b, Chart 1), which leads to three different possible environments for each proton. For compound **3** the two different isomers a and b are in a 1:12 molar ratio (see Experimental Section).

Mesomorphic Properties. The complexes were studied by optical microscopy under polarized light with a heating stage and by differential scanning calorimetry (DSC). Table 1 collects the most significant results of this study.

Notably, although the parent pyrazole ligands are not mesogenic, all the new complexes **1**−**4** show mesomorphic properties. Quite interestingly, the coordination of these binucleating ligands to gold results in the appearance of liquid crystal behavior. The observed textures of the new coordination compounds are fanlike and pseudo-focal-conic, typical of hexagonal columnar mesophases. On cooling, these derivatives exhibit a noticeable hysteresis phenomenon, probably due to

(6) Tejel, C.; Villoro, J. M.; Ciriano, M. A.; López, J. A.; Eguizabal, E.; Lahoz, F. J.; Bakhmutov, W. I.; Oro, L. A. *Organometallics* **1996**, *15*, 2967. Oro, L. A.; Pinillos, M. T.; Tejel, C.; Foces-Foces, C.; Cano, F. H. *J. Chem. Soc., Dalton Trans.* **1986**, 2193. Oro, L. A.; Pinillos, M. T.; Foces-Foces, C.; Cano, F. H. *J. Chem. Soc., Dalton Trans.* **1986**, 1087. Oro, L. A.; Pinillos, M. T.; Tejel, C.; Foces-Foces, C.; Cano, F. H. *J. Chem. Soc., Chem. Commun.* **1984**, 1687. Oro, L. A.; Carmona, D.; Lamata, M. P.; Apreda, M. C.; Foces-Foces, C.; Cano, F. H.; Maitlis, P. M. *J. Chem. Soc., Dalton Trans.* **1984**, 1823. Tiripicchio, A.; Tiripicchio-Camellini, M.; Usón, R.; Oro, L. A.; Ciriano, M. A.; Pinillos, M. T. *J. Organomet. Chem.* **1982**, *224*, 207. Usón, R.; Oro, L. A.; Ciriano, M. A.; Pinillos, M. T.; Tiripicchio, A.; Tiripicchio-Camellini, M. *J. Organomet. Chem.* **1981**, *205*, 247.

(7) Bushnell, G. W.; Fjeldsted, D. O. K.; Stobart, S. R.; Vefghy, R.; Wang, J. *Organometallics* **1996**, *15*, 3785 and references therein. Bushnell, G. W.; Stobart, S. R.; Vefghy, R.; Zaworotko, M. J. *J. Chem. Soc., Chem. Commun.* **1984**, 282.

(8) Murray, H. H.; Raptis, R. G.; Fackler, J. P. *Inorg. Chem.* **1988**, *27*, 26.

(9) Ehlert, M. K.; Rettig, S. J.; Storr, A.; Thompson, R. C.; Trotter, J. *Can J. Chem.* **1992**, *70*, 2161. Ardizzoia, G. A.; Anganoni, M. A.; La Monica, G.; Cariati, F.; Cenini, S.; Moret, M.; Masciocchi, M. *Inorg. Chem.* **1991**, *30*, 4347.

(10) (a) Minghetti, G.; Banditelli, G.; Bonati, F. *Inorg. Chem.* **1979**, *18*, 658. (b) Bovio, B.; Bonati, F.; Banditelli, G. *Inorg. Chim. Acta* **1984**, *87*, 25. Bonati, F.; Burini, A.; Pietroni, B. R.; Galassi, R. *Gazz. Chim. Ital.* **1993**, *123*, 691.

(11) La Monica, G.; Ardizzoia, G. A. *Prog. Inorg. Chem.* **1997**, *46*, 151.

(12) Barberá, J.; Giménez, R.; Serrano, J. L. *Adv. Mater.* **1994**, *6*, 470.

(13) Barberá, J.; Elduque, A.; Giménez, R.; Oro, L. A.; Serrano, J. L. *Angew. Chem., Int. Ed. Engl.* **1996**, *35*, 2832.

Table 1. Transition Temperatures (°C) and Enthalpies (kJ·mol^{-1}; in Parentheses) for Compounds **1**−**4** and Lattice Parameters for the Hexagonal Columnar Mesophases

compd	mesomorphic properties[a]			X-ray data,[b] Å
1	*K* 59 (112.1)	Col_h 64 (2.8)	*I*	32.4 (±0.2)
2	*K* 36.5[c]	Col_h 59 (5.8)	*I*	31.7 (±0.2)
3		Col_h 22 (5.9)	*I*	31.1 (±0.2)
4	*K* 35 (6.8)	Col_h 58 (4.9)	*I*	30.8 (±0.2)

[a] *K* crystal phase; Col_h hexagonal columnar mesophase; *I* isotropic liquid. [b] Calculated hexagonal lattice parameter. [c] This transition only appeared on first heating several weeks after the compound was prepared. The transition enthalpy could not be measured due to the incomplete crystallization of the sample.

the presence of a high number of long aliphatic chains. With the exception of complex **3** (see below), crystallization takes several hours, or even days, to occur, with the liquid crystal phases remaining metastable at room temperature for long periods.

Compound **1** is solid at room temperature and melts at 59 °C to form a columnar mesophase. The mesophase-to-isotropic-liquid transition (clearing point) has been detected at 64 °C. On cooling, even to −30 °C, only the isotropic liquid-to-mesophase transition is observed. The mesophase remains as a metastable state for 5 or 6 h. After this time, crystallization begins to take place very slowly. Subsequent DSC scans show a behavior analogous to that observed in the first heating/cooling process.

Freshly prepared **2** shows a columnar mesophase at room temperature and transforms into the isotropic liquid at 59 °C. After several weeks at room temperature, the DSC thermogram of **2** shows an additional peak at 36.5 °C that should correspond to the melting of a certain amount of crystalline phase not present initially.

Metal complex **3** exhibits mesomorphic behavior at room temperature. Upon heating and subsequent cooling of the samples, only a single phase transition at 22 °C could be observed under a microscope or by DSC. This structural change is clearly associated with the transition between the mesophase and the isotropic liquid. Interestingly, no subsequent crystallization of this complex was observed, either upon a decrease in temperature or after the passage of time.

On the other hand, **4** behaves as a solid at room temperature. Although its structure is poorly organized, as revealed by the low melting enthalpy, the powder X-ray study of this compound (see below) indicates that the solid phase has an essentially crystalline structure. The mesophase is stable between 35 and 58 °C, although it remains metastable for several hours at room temperature.

If we compare the thermal behaviors of the different complexes, an increase in the number of alkoxy chains (from **1** to **2**, for instance) seems to be associated with a decrease in the melting and clearing temperatures. The same effect is also observed when the symmetry of the molecule is decreased if the number of aliphatic chains is maintained (complexes **3** and **4**).

Most probably, the existence of two regioisomers for **2** and **3**, one symmetric and the other asymmetric (isomers a and b in Chart 1), hinders the local molecular homogeneity necessary for the crystalline phase to grow and causes these compounds to remain a long time in the liquid crystal state at room temperature. On the other hand, complex **1**, with three fewer aliphatic chains and no possibility of isomerism, crystallizes more easily and shows a short mesophase range in the heating process. An increase to 18 in the number of aliphatic chains—complexes **3** and **4**—leads to different results depending on their relative positions in the phenyl groups. Thus, if the alkoxy moieties are placed unsymmetrically on the central core (compound **3**), the transition temperatures decrease. However, in the case of a symmetrical arrangement of the hydrocarbon chains (**4**), an increase in the intermolecular forces seems to stabilize the crystalline phase, making it more easily accessible.

Powder X-ray Diffraction Analyses. To characterize the molecule arrangement of the different phases displayed by these gold complexes, X-ray diffraction photographs were taken for the mesophases of the four compounds at room temperature (20 °C), as well as for the solid phases of **1** and **4**. The solid-state phase of **2** could not be studied due to the failure to obtain fully crystallized samples of this complex. In some experiments, samples of **1**, **3**, and **4** were aligned (for **2** all aligning attempts were unsuccessful) by scratching the inner wall of the Lindemann glass capillaries with a small glass rod at temperatures slightly lower than the respective clearing points.

The X-ray patterns of the mesophases of these complexes (Figure 1a,c) show a set of sharp maxima in the small-angle region which correspond to reciprocal spacings in the ratio $1:\sqrt{3}:\sqrt{4}:\sqrt{7}$. These peaks were assigned to the (10), (11), (20), and (21) reflections from a two-dimensional hexagonal lattice with a lattice constant *a* of 32.4 (**1**), 31.7 (**2**), 31.1 (**3**), and 30.8 (±0.2) Å (**4**) (Table 1). These patterns are consistent with a hexagonal columnar mesophase in which the column axes are located at the nodes of the two-dimensional lattice and oriented perpendicular to the plane of this lattice.

The absence of other sharp peaks in the diffraction patterns indicates that there is not long-range order along the column axis. For this reason, reflections with Miller index $l \neq 0$ are not detected. In the large-angle region a broad diffuse halo at 4−5 Å is observed, which is related to the short-range correlations between the molten hydrocarbon chains.[14] Along with this, in the long-exposure photographs of aligned samples of **3** and **4**, a diffuse crescent is observed at middle angles in the meridian region (alignment direction) which corresponds to intracolumnar short-range correlations along the columnar axis between stacked molecules (Figure 1c). This crescent is centered at 7.5 (±0.1) Å for **3** and 7.6 (±0.1) Å for **4**. Assuming this parameter to be the mean distance between stacked molecules (*c* parameter of an ideal tridimensional packing) and assuming a *Z* value of 1, a local density could be approximated to be 1.08 g·cm^{-3} for both complexes.[15]

Compounds **1** and **4** were also studied at high temperatures either within the range of thermodynamic stability of their mesophases or at slightly lower temperatures in the cooling process. These experiments confirm that the symmetry of the mesophase found at room temperature is maintained at higher temperatures; however, an interesting contraction of the hexagonal lattice parameter *a* was observed upon heating. Thus, the lattice constant measured for **1** is 30.8 (±0.2) Å at 50 °C, 31.2 (±0.2) Å at 45 °C, and 31.6 (±0.2) Å at 40 °C. For **4**, a lattice constant of 30.1 (±0.2) Å was measured at 45 °C. In the latter compound, the shortening of the lattice parameter *a* upon heating is accompanied by an expansion of the average interdisk distance (mean *c* axis) as revealed by the shifting of the middle-angle crescent to 8.1 (±0.1) Å, probably to preserve the packing density (1.06 g·cm^{-3} was estimated for **4** at 45 °C).

(14) Levelut, A. M. *J. Chim. Phys.* **1983**, *80*, 149.

(15) The density value was estimated from the ideal equation $\rho = (M/N)/(V/Z)$, where *M* is the molar mass (g), *N* the Avogadro number, *V* the unit cell volume (cm^3), and *Z* the number of molecules per unit cell.

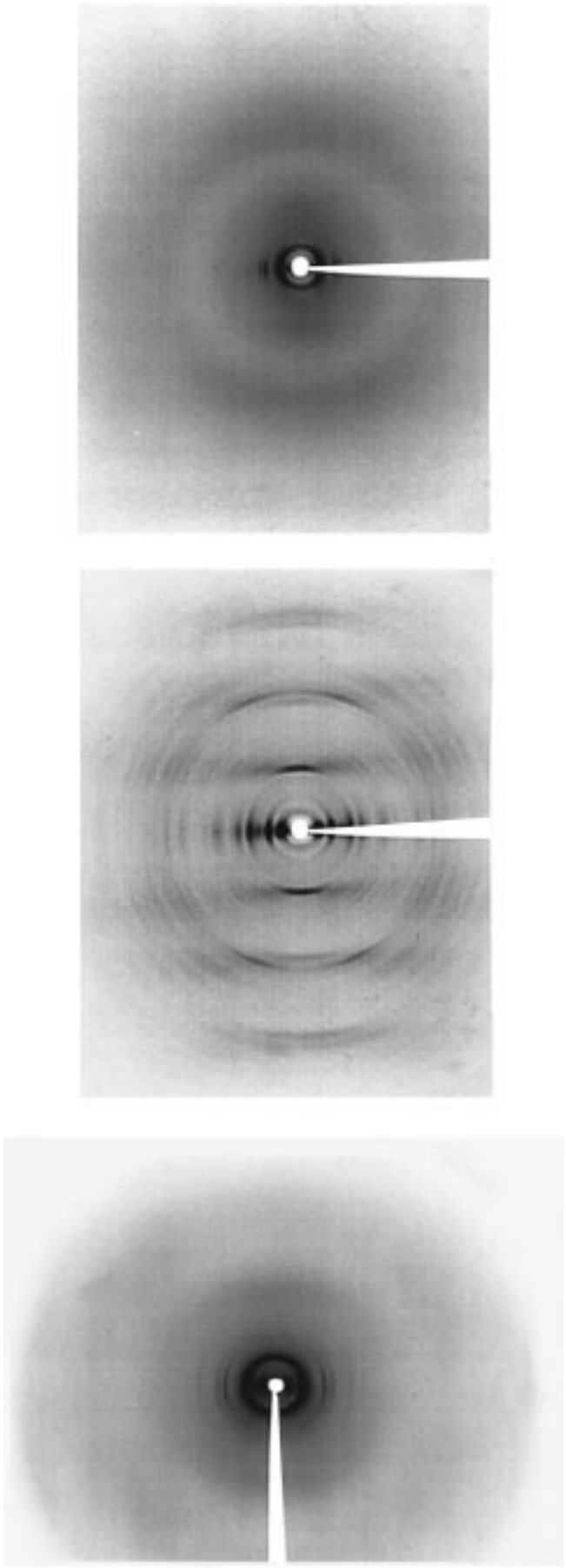

Figure 1. X-ray diffraction photographs of (a, top) the Col_h mesophase of **1**, (b, middle) the crystalline powder of **1**, and (c, bottom) the Col_h mesophase of **4**. (The sample container axis is vertical in all cases.)

It is quite remarkable that the hexagonal lattice parameters measured at room temperature are very similar for the four compounds, despite the different numbers of alkoxy groups. Furthermore, the lattice constants decrease slightly upon increasing the number of chains. This agrees with the results obtained for other columnar liquid crystals[16] and is related to an expansion in the mean intracolumnar distance as the number of hydrocarbon chains increases due to the greater spatial requirements out of the molecular plane by the longer chains. This behavior is also related to the temperature dependence of the hexagonal lattice constant for **4**: an increase in the temperature produces a shortening of the lattice constant at the expense of a lengthening of the stacking distance.

The solid phases of **1** and **4** yield more complex diffraction patterns containing numerous maxima in the whole angular range. In the case of compound **1** (Figure 1b), these maxima can be satisfactorily assigned to a three-dimensional *C*-centered orthorhombic structure, with parameters $a = 28.5$ Å, $b = 66$ Å, and $c = 9.4$ Å. A density of 1.17 g·cm^{-3} was estimated assuming $Z = 4$.[15] The powder photographs of the crystalline phase of **4** can be satisfactorily indexed in a three-dimensional hexagonal structure with parameters $a = 34.0$ Å and $c = 26.4$ Å. Assuming $Z = 4$, the calculated density is 1.02 g·cm^{-3}, a value that is in fair agreement with the density of 1.08 g·cm^{-3} estimated for the mesophase of the same compound. The lower density of compound **4** compared to that of **1** is consistent with the larger number of aliphatic chains and the smaller relative contribution of the gold atoms to the molecular mass.

Single-Crystal X-ray Analysis of [Au{3,5-(4′-MeOPh)$_2$Pz}]$_3$ (5). To acquire insight into the packing mode of these complexes and into the transformation, at molecular scale, between solid and mesomorphic phases, we attempted to obtain the crystal structure of any of the mesogenic compounds **1**−**4**. Unfortunately, we could not obtain adequate single crystals to carry out a conventional X-ray diffraction analysis. However, with this idea in mind, an analogue of **1**−**4**, with only one and a shorter aliphatic chain (methoxy group) at the phenyl ring, [Au{3,5-(4′-MeOPh)$_2$Pz}]$_3$ (**5**), was prepared using the same synthetic procedure described for **1**−**4** (eq 1). Complex **5** crystallized as white prismatic crystals. Although the obtained crystals were small and very weakly diffracting, a set of data was collected and the molecular and crystal structure of **5** evaluated.

In agreement with the mass spectroscopic data for **1**−**4**, crystals of **5** were formed by trinuclear complexes; crystallization solvent molecules (methanol) were also present in the single crystals. The diffractometric analysis showed the presence of two crystallographically independent—but chemically identical—molecules, differing slightly in the twisting of the central metallacycle core and more markedly in the relative conformation of the phenyl substituents (Figure 2). Table 2 collects the most relevant geometric bond data for both molecules, together with some torsion bond angles.

The core of the molecule is formed by three gold atoms bridged through three exobidentate pyrazolate groups, forming a nine-membered ring (Figure 2). This gold−pyrazolate macrocycle is not uncommon in the chemistry of group 11 metals; similar situations have been reported for the related (carbenato)gold(I) complex [Au{C(OEt)═N(C$_6$H$_4$Me)}]$_3$[17] or the (pyrazolato)gold(I) complexes [Au(μ-3,5-(CF$_3$)$_2$Pz)]$_3$[10b] and [Au(μ-

(16) Barberá, J.; Esteruelas, M. A.; Levelut, A. M.; Oro, L. A.; Serrano, J. L.; Sola, E. *Inorg. Chem.* **1992**, *31*, 732.
(17) Tiripicchio, A.; Tiripicchio-Camellini, M.; Minghetti, G. *J. Organomet. Chem.* **1979**, *171*, 399.

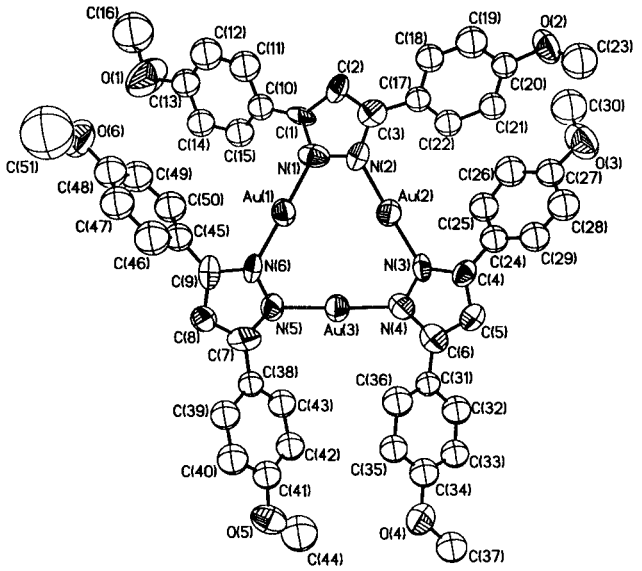

Figure 2. View of the molecular structure of one independent molecule of **5** together with the atomic numbering scheme used.

Table 2. Selected Bond Distances (Å), Angles (deg), and Torsion Angles (deg) for **5**[a]

Au(1)−N(1)	2.03(2)	2.017(18)
Au(1)−N(6)	2.01(2)	2.03(2)
Au(2)−N(2)	2.00(2)	2.02(2)
Au(2)−N(3)	2.00(2)	1.99(2)
Au(3)−N(4)	2.00(2)	2.07(2)
Au(3)−N(5)	2.01(2)	2.05(2)
Au(1)···Au(2)	3.2560(16)	3.2786(15)
Au(1)···Au(3)	3.3970(15)	3.3455(16)
Au(2)···Au(3)	3.3759(17)	3.3747(16)
N(1)−N(2)	1.40(3)	1.42(3)
N(3)−N(4)	1.37(3)	1.34(3)
N(5)−N(6)	1.34(3)	1.37(2)
N(1)−Au(1)−N(6)	177.2(8)	174.2(7)
N(2)−Au(2)−N(3)	176.4(9)	175.4(9)
N(4)−Au(3)−N(5)	176.4(10)	174.9(8)
Au(1)−N(1)−N(2)	113.6(19)	119.2(16)
Au(1)−N(1)−C(1)	135(2)	129(2)
Au(2)−N(2)−N(1)	118.3(19)	115.8(17)
Au(2)−N(2)−C(3)	133.0(19)	134(2)
Au(2)−N(3)−N(4)	120.5(17)	120.4(18)
Au(2)−N(3)−C(4)	129(2)	134(2)
Au(3)−N(4)−N(3)	119.4(18)	118.4(19)
Au(3)−N(4)−C(6)	133(2)	128(2)
Au(3)−N(5)−N(6)	117.7(18)	116.0(16)
Au(3)−N(5)−C(7)	131(2)	135(2)
Au(1)−N(6)−N(5)	123.6(17)	119.3(16)
Au(1)−N(6)−C(9)	125(2)	128.0(19)
Au(1)−N(1)−N(2)−Au(2)	25(2)	1(2)
Au(2)−N(3)−N(4)−Au(3)	6(3)	−18(3)
Au(3)−N(5)−N(6)−Au(1)	7(3)	24(2)

[a] The two values presented correspond to the two crystallographic independent molecules.

3,5-Ph_2Pz)]$_3$,[8] for the heterovalent Au(I)/Au(III) compounds [{Au(μ-3,5-Ph_2Pz)}$_3Cl_2$] and [{Au(μ-3,5-Ph_2-4-ClPz)}$_3Cl_2$],[18,19] and for the closely related silver(I) analogue [Ag(μ-3,5-Ph_2-Pz)]$_3$.[8] In **5**, as in all the previous structures (except [Au(μ-3,5-Ph_2Pz)]$_3$, which exhibits intramolecular crystallographically imposed symmetry), the metallacycle is not strictly planar, but slightly irregular and puckered. The nitrogen atoms of the pyrazolate ligands are out of the plane defined by the three gold atoms up to 0.51(2) Å. The phenyl rings are rotated with respect to the Au_3 plane by 29.6(6)−68.0(7)°. Assuming free rotation of the phenyl rings, the molecules exhibit a roughly D_{3h} overall symmetry. As a whole, the full molecule shows a nearly triangular-planar shape, a direct consequence of the bonding system established between the metal and the pyrazolate ligands (Figure 3).

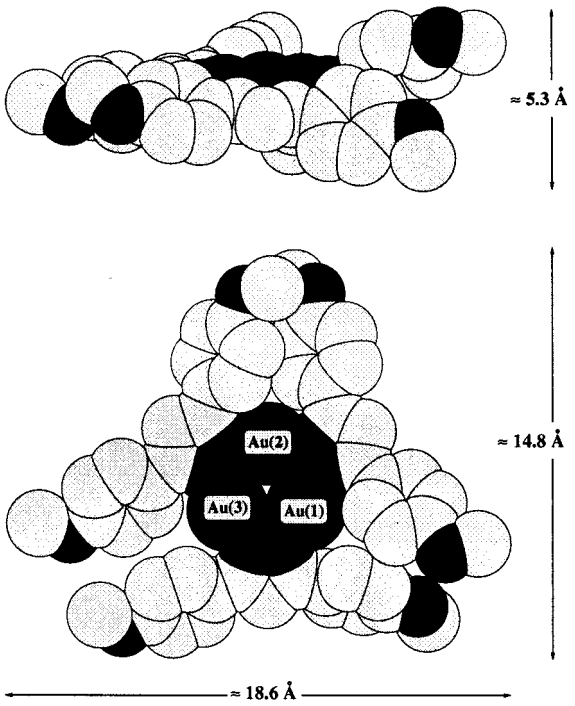

Figure 3. Space-filling representation of **5** showing approximate molecular dimensions and the overall triangular-planar shape of the molecule.

The three metal atoms present two-coordinate linear gold(I) arrangements. The N−Au−N bond angles range between 174.9(8) and 177.2(8)°. In the trimers, the Au···Au mean distances of 3.3380(7) Å (range 3.2560(16)−3.3970(15) Å) are much longer than that in metallic gold (2.884 Å)[20] but close to the values observed in the phenyl-substituted gold(I) complex [Au(μ-3,5-Ph_2Pz)]$_3$ (3.368(1) Å)[8] or gold(I)/gold(III) complexes [{Au(μ-3,5-Ph_2Pz)}$_3Cl_2$] (3.334−3.383(1) Å)[18] and [{Au(μ-3,5-Ph_2-4-ClPz)}$_3Cl_2$] (3.3352−3.4011(7) Å).[19] Most likely, a feeble intramolecular gold−gold bonding interaction is present, as all the distances are shorter than the calculated value (ca. 3.4 Å) for a planar nine-membered metallacycle. The observed intermolecular Au···Au distances (≥4.252 Å) suggest that metal−metal interactions do not play an important role in the packing of **5** in the solid state.

The observed N−Au lengths range between 1.99(2) and 2.07(2) Å, with mean values of 2.01 and 2.03(1) Å for both independent molecules. These values are longer than those reported for the CF_3 analogue,[10b] 1.93(3) Å, but statistically indistinguishable from the Au−N bond distances described in complexes containing phenyl-substituted pyrazolate ligands (range 1.978(9)−2.05(2) Å).[8,18,19] The pyrazolate rings and the phenyl groups maintain strict planarity and do not deserve further comment.

The most remarkable feature of this crystal structure is the packing mode observed. This arrangement is governed by van der Waals forces and seems to be related to the overall triangular planar shape of the molecules (Figure 3). The trimers pack

(18) Raptis, R. G.; Murray, H. H., Fackler, J. P., Jr. *Acta Crystallogr.* **1988**, *C44*, 970.
(19) Raptis, R. G.; Fackler, J. P., Jr. *Inorg. Chem.* **1990**, *29*, 5003.
(20) Jones, P. G. *Gold Bull.* **1981**, *14*, 102.

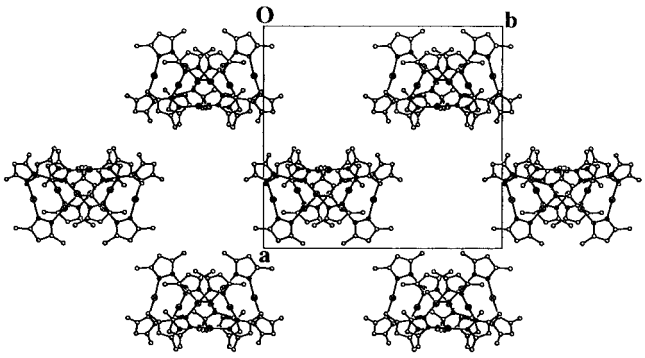

Figure 4. View of the crystal structure of **5** along the *c* axis showing the columnar arrangement present in the solid state. For clarity, only the C_{ipso} carbons of the methoxyphenyl substituents of the pyrazolate ligands are represented.

together in apparent and definite columnar arrangements parallel to the crystallographic *c* axis, with small displacements of the molecule centroids from the columnar axis. Figure 4 shows a simplified view of the packing organization along the columnar axis and the relative disposition to this axis of the different molecules (four) that form the columns. From the measurement of the lattice parameter *c* (parallel to the columnar axis), the mean stacking separation between two consecutive trimers could be evaluated to be approximately 4.54 Å (18.174/4), a typical intermolecular distance in disklike molecules.[14]

Relationship between the Molecular Packings in the Crystal Structures and in the Mesophases. The crystal structure of **5** offers a clear example to outline the relationship between the solid-state and the mesophase molecular arrangements for complexes **1**−**4**. Controlling the metal coordination sphere and the coordinative ability of the pyrazolate ligands, we have been able to prepare trinuclear—roughly triangular-planar (Figures 2 and 3)—complexes (**1**−**5**). As a consequence of this tailored molecular shape, the supramolecular arrangements are built from columns of stacked trimers that could adopt different relative dispositions (Figure 4), leading to diverse crystallization systems and/or space groups but always maintaining clear columnar arrangements.

The tendency of this type of molecules to stack into columns, not only in the mesophase but also in the crystalline state, can be clearly seen if we analyze carefully the results obtained from the X-ray powder experiments. For the orthorhombic structure of **1** the area per molecule in the *ab* plane must be 940 Å^2 (28.5 Å × 66 Å/2), a value that compares well with the area per molecule calculated in the mesophase at room temperature, 909 Å^2 (32.4 Å × 32.4 Å × ($\sqrt{3}$)/2). This, together with the fact that the *c* parameter is much shorter than *a* and *b*, suggests that the molecules lie approximately in the *ab* plane and stack along the *c* axis also in the solid state. It must be pointed out that the direction of the short axis (*c* axis) is preserved upon transition from the mesophase to the solid (vertical direction in Figure 1). As the unit cell for **1** is *C*-centered, two molecules are located at + 0, 0, 0 and + $^1/_2$, $^1/_2$, 0, and the two additional ones should be disposed along *c* axis giving rise to a mean stacking distance of 9.4 Å/2 = 4.7 Å, a value that is within the range of typical intermolecular distances in disklike molecules[14] and compares well with the mean separation between two consecutive complex molecules deduced from the single-crystal analysis of compound **5**. Under the assumption that the density value calculated for **1** in the solid state is maintained in the mesophase at room temperature (1.17 g·cm^{-3}), it could be possible to estimate, through the unit cell volume,[15] a reasonable value for the *c* constant of the hexagonal unit cell in the columnar mesophase. The obtained value, 4.87 Å, should correspond to the mean interdisk distance, and it compares well with the stacking distance of 4.7 Å found in the solid state. Most probably, the corresponding diffraction maximum at 4.87 Å could not be observed in the mesophase X-ray pattern as it is overlapped with the broad 4−5 Å halo arising from the interchain correlations.

Although the lack of crystal data for compound **2** precludes a similar estimation of the mean stacking distance, we can reasonably assume that its density at room temperature must be around 1.1 g·cm^{-3} (an intermediate value between the density of **1** and the densities of **3** and **4**). In this way, the *c* constant was estimated to be 6.2 Å approximately.[15] The corresponding maximum could not be observed in the X-ray photograph probably due to its diffuseness (the intracolumnar order extends only to very short distances) together with the failure to obtain oriented patterns of this compound.

In the crystalline structure of **4**, the area per molecule has been calculated to be 1001 Å^2 (34 Å × 34 Å × ($\sqrt{3}$)/2), a value significantly larger than the molecular area obtained in the mesophase, 822 Å^2 (30.8 Å × 30.8 Å × ($\sqrt{3}$)/2). As the direction of the *c* axis seems to be preserved upon transition from the mesophase to the solid state, analogous to the case of compound **1**, it can be concluded that in the crystal phase the molecules of **4** lie approximately in the (001) plane and stack along the *c* axis. Assuming $Z = 4$, it is deduced that four molecules are stacked in the unit cell at a mean distance of 26.4 Å/4 = 6.6 Å. The larger molecular area and lattice constant *a*, as well as the shorter stacking distance in the solid compared to the liquid crystal structure (7.6 Å), indicate that the hydrocarbon chains are more extended in the solid state, in contrast to the conformational freedom in the mesophase. As the temperature increases, the thermal displacement of all atoms should be intensified, affecting to a major extent the external part of the molecules, that is, fundamentally to the atoms of the aliphatic chains. This increase in the flexibility of the outer part of the trimers should modify the overall shape of the trimers toward a more disklike appearance (circular shape). Eventually, the formed cylindrical columns are ordered toward the best space-saving packing alternative, that is, the hexagonal columnar array. The transition from the crystal to the liquid crystal phase involves translational decorrelation of neighboring columns and loss of long-range order along the stacking axis. Simultaneously, if we compare the cell parameters in the solid and in the mesophase, a distortion of the distances occurs in the plane perpendicular to the *c* axis. In compound **1**, the transition involves a lengthening of the orthorhombic lattice along the *a* axis and a shortening along the *b* axis, to give the ratio $b/a = \sqrt{3}$ characteristic of a hexagonal structure.[13] In compound **4**, the transition does not imply a symmetry change but involves a shortening of the *a* constant accompanied by an increase in the mean interdisk distance.

Conclusions

This paper has shown the tailored use of pyrazolate ligands and metal coordination spheres as building motifs for the construction of complexes of previously determined molecular structures. All the complexes investigated in the series display columnar mesomorphism, and their molecules show a tendency to stack into columns not only in the mesophase but also in the crystalline state. The presence of columnar arrangements already in the solid phase has been confirmed by the X-ray study of a single crystal of the closely related short-chain complex **5**.

Chart 2

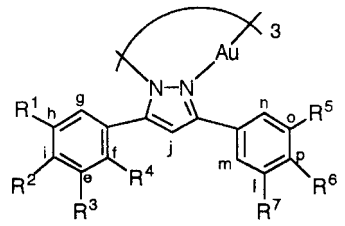

R^1-R^7 = H or $\overset{a}{CH_3}$-$(\overset{b}{CH_2})_7$-$\overset{c}{CH_2}$-$\overset{d}{CH_2}$-O or $\overset{a}{CH_3}$O

Table 3. Crystallographic Data for [Au{3,5-(4′-MeOPh)$_2$Pz}]$_3$ (**5**)

empirical formula	$C_{51}H_{45}Au_3N_6O_6 \cdot {}^1/_2CH_3OH$
fw	1444.85
cryst size, mm	0.42 × 0.18 × 0.18
temp, K	293(1)
cryst system	monoclinic
space group	$P2_1/c$ (No. 14)
a, Å	23.185(3)
b, Å	23.843(3)
c, Å	18.174(3)
β, deg	104.777(8)
V, Å^3	9714(2)
Z	8
ρ(calcd), g·cm^{-3}	1.976
μ(Mo Kα), mm^{-1}	9.096
θ range, deg	1.8−21.0
hkl ranges	−23 to +22, −24 to +1, −1 to +18
no. of collected reflcns	11 609
no. of unique reflcns	10 305 (R_{int} = 0.0561)
min, max transm factors	0.014, 0.029
data/restraints/parameters	10305/3/790
$R(F)$ [$F^2 > 2\sigma(F^2)$][a]	0.0577
$R_w(F^2)$ [all data][b]	0.1448
S [all data][c]	1.031

[a] $R(F) = \sum(|F_o| - |F_c|)/\sum|F_o|$, for 5502 observed reflections. [b] $R_w(F^2) = (\sum[w(F_o^2 - F_c^2)^2]/\sum[w(F_o^2)^2])^{1/2}$. [c] $S = [\sum[w(F_o^2 - F_c^2)^2]/(n - p)]^{1/2}$; n = number of reflections, p = number of parameters.

These columnar arrangements are maintained in the mesophase where the intercolumnar relative disposition adopts a hexagonal symmetry.

It is also interesting to note that the reported mesogenic gold complexes constitute the first examples of trinuclear metal-containing liquid crystals obtained by coordination of nonmesogenic bridging ligands.

Experimental Section

All reactions were carried out under a N_2 atmosphere using Schlenk techniques. The solvents were dried and freshly distilled. [AuCl(tht)],[21] 3,5-bis(3′,4′-di-*n*-decyloxyphenyl)pyrazole (**pz1**), 3-(3′,4′,5′-tri-*n*-decyloxyphenyl)-5-(3″,4″-di-*n*-decyloxyphenyl)pyrazole (**pz2**), 3-(2′,3′,4′-tri-*n*-decyloxyphenyl)-5-(3″,4″,5″-tri-*n*-decyloxyphenyl)pyrazol (**pz3**), and 3,5-bis(3′,4′,5′-tri-*n*-decyloxyphenyl)pyrazole (**pz4**)[22] were prepared by literature methods. All compounds were characterized satisfactorily by elemental analysis, ^{1}H NMR and IR spectroscopy, and mass spectrometry. Microanalyses were performed with a Perkin-Elmer 240C microanalyzer. ^{1}H NMR spectra were recorded on a Varian Unity 300 spectrometer. IR spectra were obtained on a Perkin-Elmer 1600 (FTIR series) spectrometer. Mass spectra were obtained on a VG Autospec EBE (FAB$^+$, 3-NBA matrix). The optical textures of the mesophases were observed with an Olympus polarizing microscope equipped with a Linkam THMS 600 heating−cooling stage and a TMS 91 central processor. The transition temperatures were measured by differential scanning calorimetry with a TA Instruments 2000 calorimeter operated at a scanning rate of 10° min^{-1}. The apparatus was calibrated with indium (156.6 °C, 28.4 J g^{-1}) as the standard. Powder X-ray diffraction patterns were obtained using a Pinhole camera (Anton-Paar) operating with a point-focused Ni-filtered Cu Kα beam. The sample was held in Lindemann glass capillaries (1 mm diameter) and heated, when necessary, with a variable-temperature attachment. The diffraction patterns were collected on flat photographic films.

Preparation of the [Au(pz)]$_3$ Complexes 1−5. Complexes **1**−**5** were prepared by the following general method: A solution of potassium pyrazolate (prepared "in situ" by reaction of an acetone solution (20 mL) of pyrazole (0.312 mmol) and KOH in methanol (1 mL, 0.320 M)) was added dropwise to a suspension of [AuCl(tht)] (100 mg, 0.312 mmol) in acetone (10 mL). The reaction mixture was stirred for 5 h (**1** and **2**), 12 h (**3** and **4**), or 2 h (**5**), and the solvents were evaporated to dryness. Addition of methanol (10 mL) and filtration through Kieselguhr led to a colorless solution. Concentration of the solution to ca. 1 mL and addition of a mixture of diethyl ether (1 mL) and methanol (10 mL) gave a solid, which was separated by filtration, washed with methanol, and vacuum-dried.

[Au(pz1)]$_3$ (1). Compound **1** was isolated as a white solid and further purified by column chromatography, hexane/dichloromethane 4/1, giving a white microcrystalline product. Yield: 40%. Anal. Calc (found) for $C_{165}H_{273}N_6Au_3O_{12}$: C, 63.44 (63.13); H, 8.81 (8.69); N, 2.69 (2.64). ^{1}H NMR (in $CDCl_3$, 55 °C): δ = 0.83−0.87 (m, 36H, Ha), 1.24−1.47 (m, 168H, Hb), 1.70−1.80 (m, 24H, Hc), 3.74 (t, J = 6.4 Hz, 12H, Hd, meta), 3.92 (t, J = 6.4 Hz, 12H, Hd, para), 6.51 (d, J = 8.2 Hz, 6H, He, Hl), 6.74 (s, 3H, Hj), 7.21 (d, J = 1.8 Hz, 6H, Hg, Hn), 7.38 (dd, J = 8.2 Hz, J = 1.8 Hz, 6H, Hf, Hm). (See Chart 2 for labeling of hydrogen atoms.) IR (Nujol, NaCl pellet): ν(C═N and ar C═C) 1607, 1589, 1528, 1501 cm^{-1}; ν(C−O) 1261 cm^{-1}. MS (FAB$^+$), *m*/*z*: 3123 ([M$^+$ − H]). MW (calc (found)): 3124.0 (3020.0).

[Au(pz2)]$_3$ (2). Compound **2** was isolated as a colorless waxy product and was purified by column chromatography, hexane/dichloromethane 4/1. Yield: 35%. Anal. Calc (found) for $C_{195}H_{333}N_6Au_3O_{15}$: C, 65.19 (65.42); H, 9.34 (8.96); N, 2.34 (2.37). ^{1}H NMR (in $CDCl_3$, 55 °C): δ = 0.84−0.89 (m, 45H, Ha), 1.26−1.49 (m, 210H, Hb), 1.65−1.79 (m, 30H, Hc), 3.59−3.92 (4t, 30H, Hd), 6.44, 6.45, 6.51, and 6.52 (4d, J = 8.4 Hz, 3H, Hl), 6.74, 6.75, 6.77, and 6.79 (4s, 3H, Hj), 6.96, 6.98, 7.05, and 7.06 (4s, 6H, Hg, Hf), 7.18, 7.21, 7.22, and 7.26 (d, J = 2 Hz, 3H, Hn), 7.37−7.44 (m, 3H, Hm). IR (Nujol, NaCl pellet): ν(C═N and ar C═C) 1586, 1524, 1494 cm^{-1}; ν(C−O) 1259, 1239 cm^{-1}. MS (FAB$^+$), *m*/*z*: 3593 (M$^+$). MW (calc (found)): 3592.8 (3432.8).

[Au(pz3)]$_3$ (3). Compound **3** was isolated as a colorless oil and was purified by column chromatography, hexane/dichloromethane 5/1. Yield: 34%. ^{1}H NMR (in $CDCl_3$, 55 °C): δ = 0.82−0.87 (m, 54H, Ha), 1.20−1.49 (m, 252H, Hb), 1.65−1.74 (m, 36H, Hc), 3.45 (m, 9H, Hd), 3.78−3.96 (m, 27H, Hd), 5.98, 6.11, and 6.12 (3d, J = 8.6 Hz, 3H, Hh), 6.87, 6.93, and 7.00 (3s, 3H, Hj), 6.89, 7.02, and 7.03 (3s, 6H, Hm, Hn), 7.28, 7.31, and 7.54 (3d, J = 8.6 Hz, 3H, Hg). IR (Nujol, NaCl pellet): ν(C═N and ar C═C) 1583, 1484 cm^{-1}; ν(C−O) 1237 cm^{-1}.

[Au(pz4)]$_3$ (4). Compound **4** was isolated as a colorless waxy product and was purified by column chromatography, hexane/dichloromethane 5/1. Yield: 32%. Anal. Calc (found) for $C_{225}H_{393}N_6Au_3O_{18}$: C, 66.54 (66.63); H, 9.75 (9.51); N, 2.07 (2.03). ^{1}H NMR (in $CDCl_3$, 55 °C): δ = 0.82−0.89 (m, 54H, Ha), 1.23−1.49 (m, 252H, Hb), 1.59−1.70 (m, 36H, Hc), 3.55 (t, J = 6.2 Hz, 24H, Hd meta), 3.88 (t, J = 6.5 Hz, 12H, Hd para), 6.83 (s, 3H, Hj), 7.01 (s, 12H, Hf, Hg, Hm, Hn). IR (Nujol, NaCl pellet): ν(C═N and ar C═C) 1600, 1583, 1486 cm^{-1}; ν(C−O) 1241 cm^{-1}. MS (FAB$^+$), *m*/*z*: 4061([M$^+$ − 1]).

[Au{3,5-(4′-MeOPh)$_2$Pz)]$_3$ (5). Compound **5** was isolated as a white solid and further purified by column chromatography, hexane/dichloromethane 4/1, giving a white microcrystalline product. Yield: 60%. Anal. Calc (found) for $C_{51}H_{45}N_6Au_3O_6$: C, 42.87 (42.86); H, 3.17 (2.91); N, 5.88 (5.77). ^{1}H NMR (in $CDCl_3$): δ = 3.77 (s, 18H, Ha), 6.62 (d, J = 8.8 Hz, 12H, He, Hh, Hl, Ho), 6.75 (s, 3H, Hj), 7.67 (d, J = 8.8 Hz, 12H, Hf, Hg, Hm, Hn).

X-ray Structural Analysis of [Au{3,5-(4′-MeOPh)$_2$Pz)]$_3$ (5). A summary of crystal data and refinement parameters is given in Table

(21) Usón, R.; Laguna, A.; Laguna, M. *Inorg. Synth.* **1989**, *296*, 85.
(22) Barberá, J.; Cativiela, C.; Serrano, J. L.; Zurbano, M. M. *Liq. Cryst.* **1992**, *11*, 887.

3. A white prismatic block was mounted on the top of a glass fiber, and a set of randomly searched reflections were indexed to monoclinic symmetry. Data were collected on a Siemens P4 four-circle diffractometer with graphite-monochromated Mo Kα radiation, using the $\omega/2\theta$ scan method. A set of three standard reflections were monitored every 100 measured reflections throughout data collection; the observed decay (3.3%) was corrected according to the intensity of the standards. All data were corrected for Lorentz and polarization effects and for absorption using a semiempirical method.[23]

The structure was solved by direct methods[24] and Fourier techniques and refined by full-matrix least-squares calculations on F^2 (SHELXL-97).[25] Anisotropic displacement parameters were used in the last cycles of refinement for Au, O, N, and pyrazolate carbon atoms. Hydrogen atoms for the pyrazolate and phenyl rings were introduced in calculated positions (C−H = 0.97 Å) and refined riding on the corresponding carbon atoms. Weighting scheme used: $w = 1/[\sigma^2(F_o^2) + (xP)^2 + yP]$ ($P = (F_o^2 + 2F_c^2)/3$) with $x = 0.0504$ and $y = 46.7808$. Maximum and minimum residual peaks in the final difference map were 1.04 and −0.86 e·Å^{-3}. Atomic scattering factors, corrected for anomalous dispersion, were used as implemented in the refinement program.

(23) North, A. C. T.; Phillips, D. C.; Mathews, F. S. *Acta Crystallogr., Sect. A* **1968**, *24*, 351.
(24) Altomare, A.; Cascarano, G.; Giacovazzo, C.; Guagliardi, A. *J. Appl. Crystallogr.* **1994**, *27*, 435.
(25) Sheldrick, G. M. *SHELXL-97*; University of Göttingen: Göttingen, Germany, 1997.

Acknowledgment. We thank the DGICYT (Project PB94-1186; Programa de Promoción General del Conocimiento) and CICYT (Project MAT-97-0986-C02-01) for financial support and the Diputación General de Aragón for a research studentship to R.G.

Supporting Information Available: A fully labeled ORTEP plot for the second independent molecule of **5** (1 page). An X-ray crystallographic file, in CIF format, for complex **5** is available on the Internet only. Ordering and access information is given on any current masthead page.

IC971632Y